The Effects of Thermal Treatment on the Properties and Performance of Hot Extruded Zn-Based Bioresorbable Alloy for Vascular Stenting Applications

Henry D. Summers, Morteza S. Ardakani, and Jaroslaw W. Drelich

Abstract A new series of zinc alloys is in development for bioresorbable stent implantation to alleviate the current materials' long-term complications. Characterization and optimization of the microstructure and corresponding mechanical properties during manufacturing stages will help researchers meet the required values. In this study, the effect of hot extrusion on the Zn-Ag-Mn-Cu-Zr-Ti alloy is characterized. Additionally, thermal treatments at 390 °C for 15, 25, 40, 60, and 120 min were performed to evaluate the effect of intermetallic phase fractions on the corrosion resistance and mechanical strength. Quantitative analysis of X-ray diffraction data demonstrates that the fractions of the $MnZn_{13}$, $ZrZn_{22}$, and $Zn_{0.75}Ag_{0.15}Mn_{0.10}$ intermetallic phases decrease as the thermal treatment time increases. Corrosion tests reveal a reduction in the corrosion rate of the extruded alloy after thermal treatment. The results of uniaxial compression tests and tensile tests show lower strength and higher ductility in all heat-treated conditions compared with the as-extruded condition.

Keywords Zinc alloys · Biodegradable stent · Corrosion behavior · Mechanical properties

Introduction

Bioresorbable metals have received significant attention over the last several decades as candidates for temporary stents to alleviate long-term complications associated with traditionally used materials. Stent implantation is most commonly performed with the use of permanent metallic stents, composed of austenitic stainless steel, Ti-Ni alloys, and Co-Cr alloys [1]. These materials are suitable candidates for stenting due to their high strength and resistance to corrosion, however, they present challenges

H. D. Summers · M. S. Ardakani · J. W. Drelich (✉)
Department of Materials Science and Engineering, Michigan Technological University, Houghton, MI 49931, USA
e-mail: jwdrelic@mtu.edu

The Minerals, Metals & Materials Society, *TMS 2023 152nd Annual Meeting & Exhibition Supplemental Proceedings*, The Minerals, Metals & Materials Series,
https://doi.org/10.1007/978-3-031-22524-6_26

such as inflammatory reactions, late stent thrombosis, and in-stent restenosis [1, 2]. Additionally, permanent stents remain in the body for their lifetime in spite of the fact that they are needed only for several months to complete their task as vascular scaffolding. Bioresorbable metallic stents will be broken down, metabolized, and harmlessly excreted by the body after providing mechanical support to widened blood vessels for 4–6 months.

The conditions a stent undergoes during implantation and service require not only high strength and ductility, but its corrosion rate must also be optimized to ensure premature degradation does not occur, without hindering its ability to degrade into the body after completion of its role as arterial scaffolding. Over the last several decades, exploratory and pre-clinical research in this area has primarily focused on bioresorbable stents made of either polymers or magnesium (Mg) alloys [1, 3]. Polymeric stents, despite their predictable degradation behavior and acceptable biocompatibility, require a greater strut thickness than metal stents due to their poor mechanical properties and low radial strength [4, 5]. This reduces the flexibility of the stents and restricts access to narrower vessels. Although biocompatible Mg-based alloys have better mechanical properties, due to the rapid corrosion behavior of magnesium, they have been found to be inadequate alternatives for many applications [6, 7].

Zinc (Zn)-based alloys have been introduced as desirable candidates for stenting due to their excellent biocompatibility and corrosion uniformity [8, 9]. Although the ultimate tensile strength of pure Zn is far lower than the benchmark required for vascular stenting, nontoxic low-content alloying additions such as silver (Ag), copper (Cu), and titanium (Ti) have been proven to improve its strength, particularly when paired with thermomechanical processing that promotes refinement of microstructure such as extrusion [9]. Additionally, manganese (Mn) has been shown to drastically improve the elongation of pure Zn [10].

The primary purpose of this study is to investigate the microstructural evolution that results from hot extrusion and thermal treatment of a novel senary Zn-based alloy containing Ag, Cu, Mn, Zr, and Ti. Samples of this alloy in the form of ingots and hot extruded rods are cross-sectioned and analyzed with electron microscopy for typical grain sizes and phase identification, including fine precipitates, produced in the material at manufacturing conditions. The rods are also subjected to thermal treatments in an effort to refine their microstructure and optimize their mechanical and corrosion properties. Mechanical testing is used to characterize the effects of different thermal treatments on the strength and ductility of the alloy and electrochemical techniques are performed to provide insight into the corrosion behavior before and after treatment. The sections that follow describe the experimental procedures, results, and discussion of the results, and the conclusions that can be drawn from this study.

Experimental Procedures

Materials and Processing

Here, the response to the thermal treatment of a novel Zn-2.77Ag-0.76Mn-0.50Cu-0.11Zr-0.03Ti alloy is investigated. A cast ingot, 500 mm in diameter, and an extruded rod 12.6 mm in diameter were cast and extruded by Fort Wayne Metals Research Products, LLC. Heat treatment of the extruded rod was conducted at 390 °C for the following durations: 10, 15, 25, 40, 60, and 120 min.

Microstructural Characterization

Samples of the as-cast ingot and extruded rod, in both the as-extruded and heat-treated conditions, were cross-sectioned (perpendicular to the direction of extrusion in the case of the rod) and mounted in epoxy. Samples were ground and polished following standard mechanical polishing procedure and etched in a 3% nital solution. Backscattered electron (BSE) scanning electron microscopy (SEM) was used to observe the microstructural evolution after the various thermal treatments. Grain size distributions were obtained from the SEM images using the Olympus Stream image analysis software (version 2.4.2).

X-ray diffraction (XRD) was used to identify intermetallic phases present within the microstructure of the material and to evaluate the quantitative changes in the content of these phases resulting from the various heat treatment durations. Samples were prepared for XRD with the same process of grinding and polishing previously described, however, the final stage of polishing and subsequent etching was repeated a total of three times before breaking the samples out of the epoxy. The data were collected with an XDS-2000 θ-θ diffractometer with CuKα radiation (Kα = 1.540562 Å) operating at −45 kV and 35 mA, from $2\theta = 20°$ to 90° with a 0.02° step size. MDI JADE software (version 8.5) was used for both peak identification and quantitative phase analysis.

Mechanical Testing

Tensile bars and cylindrical compression test samples were machined from the extruded rod with the long axis parallel to the direction of extrusion. The tensile bars were machined to a gauge length of 16 mm and a diameter of 4 mm, and the compression samples to a height of 10 mm and diameter of 4 mm. Tensile bars were heat-treated at 390 °C for durations of 10, 15, and 25 min and the compression samples were heat-treated at the same temperature for 15, 25, 40, 60, and 120 min. As-extruded samples were tested in both experiments as well. Both the tensile and

compression tests were performed using an MTS Instron 4206 load frame at room temperature with an initial strain rate of 1×10^{-3} s^{-1} in accordance with ASTM E8-04 [11] and ASTM E9-19 [12], respectively. Due to the limited supply of the extruded rod available, only one tensile test was performed for each of the heat treatment conditions. Standard deviation was calculated for the compression tests from a population of two experiments, however, only one trial was performed for the 60-min and 120-min heat treatment conditions due to material supply constraints.

Corrosion Testing

The corrosion resistance of the extruded rod was characterized before and after the 15-min heat treatment by potentiodynamic corrosion testing in a three-electrode cell using a Princeton Applied Research PARSTAT 4000 potentiostat/galvanostat measurement system in accordance with ASTM G59-97 [13]. The tests were carried out in a modified Hank's salt solution with a scanning rate of 0.166 mV/s and an applied potential ranging from −1.5 to −0.2 mV, based on previous studies [14]. The test solution was prepared through the addition of 9.8 g Hank's balanced salts (H1387) and 0.35 g $NaHCO_3$ to 1 L of distilled water. This solution was brought to a pH of 7.4 through the addition of 1 M HCl or 1 M NaOH as necessary and held at a temperature of 37 ± 2 °C during testing. The samples were mounted in epoxy and polished to 0.25 μm. After the final polishing step, the samples were washed in an ultrasonic bath of ethanol for five minutes and then tested immediately after drying to mitigate surface oxidation. The corrosion rate was calculated from the corrosion current density (i_{corr}) obtained with Tafel extrapolation using

$$CR = 3.27 * 10^{-3} * \frac{i_{corr} * EW}{\rho} \quad (1)$$

where CR is the corrosion rate (mm/year), i_{corr} is the corrosion current density ($\mu A/cm^2$), EW is the equivalent weight, which is 32.6 for pure zinc, and ρ is density (g/cm^3). Corrosion rates are reported as the mean values with standard deviation calculated from 3 experiments for each sample condition.

Results and Discussion

Microstructural Characterization

The microstructures of the Zn-Ag-Mn-Cu-Zr-Ti alloy in the as-extruded and heat-treated conditions are displayed in Fig. 1, along with the grain size distributions and average grain sizes. The average grain size for the as-cast ingot was found to be 70

$\pm$ 40 μm. Substantial refinement of grain size is observed from the as-cast ingot to the as-extruded rod (a reduction in average grain size of approximately 87% from hot extrusion). Heat treatment of the extruded rod results in increasing average grain size as the duration is extended. After 120 min at 390 °C, the average grain diameter increased 16% from the as-extruded state.

Evaluation of the microstructural evolution from extrusion and heat treatment also revealed the presence of three different intermetallic phases using energy dispersive spectroscopy (EDS). EDS shows that there are distinct phases rich in manganese,

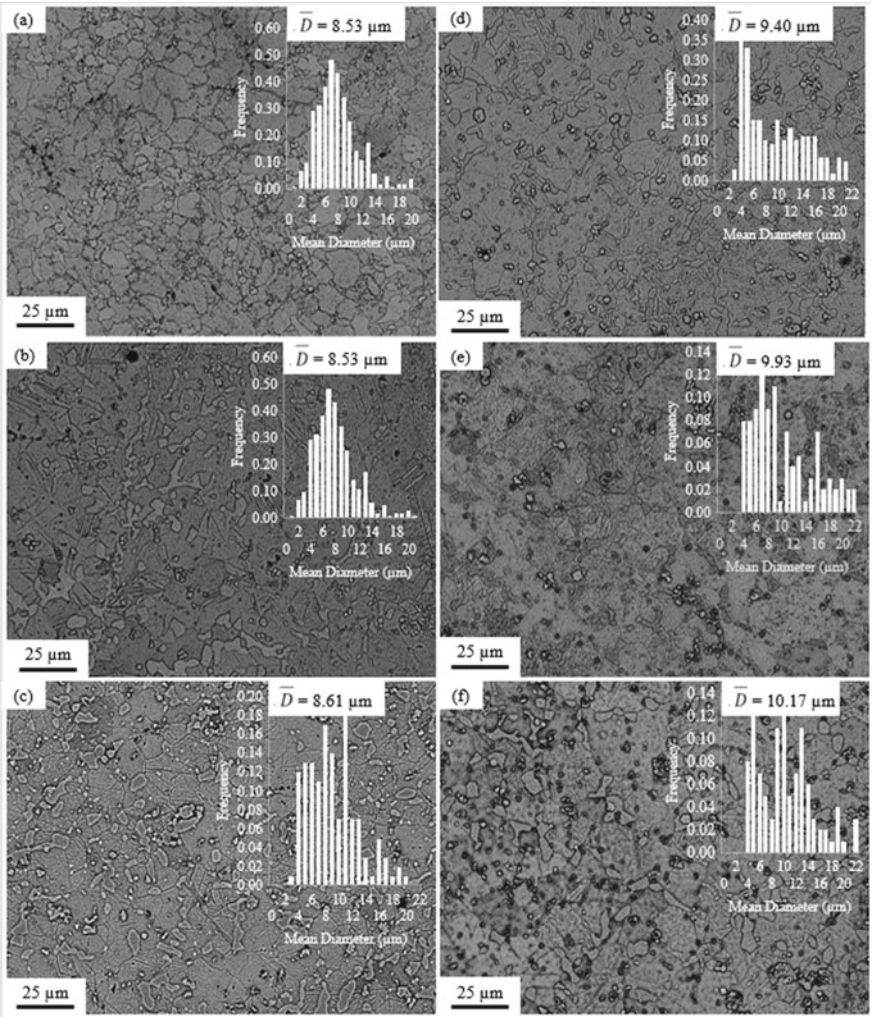

Fig. 1 SEM-BSE images of microstructure, grain size distributions, and average grain size ($\bar{D}$) for the extruded rod in the **a** as-extruded state and after heat treatment durations of **b** 15 min, **c** 25 min, **d** 40 min, **e** 60 min, and **f** 120 min

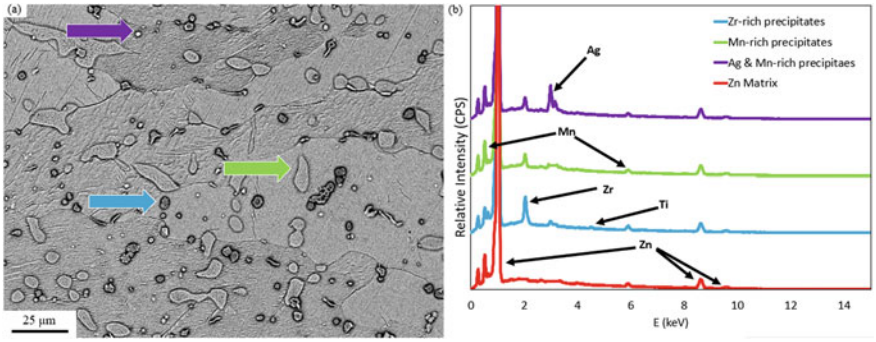

Fig. 2 **a** SEM-BSE image of as-extruded rod microstructure with green, blue, and purple arrows corresponding to intermetallic precipitates rich in Mn, Zr, and Ag, respectively, and **b** EDS spectra of these phases

zirconium, and a combination of manganese and silver. Silver appears to be present to some extent in the EDS spectra of all identified phases, likely due to its high weight fraction relative to other alloying elements, and its solubility in the zinc matrix. Intermetallic phases rich in Mn, Zr, and Ag are displayed in Fig. 2 with green, blue, and purple arrows, respectively. Analysis of X-ray diffraction data (Fig. 3a) reveals two intermetallic phases in the as-cast ingot, and three in the extruded rod (in both as-extruded and heat-treated states). The intermetallic phases $ZrZn_{22}$ and $Zn_{0.75}Ag_{0.15}Mn_{0.10}$ were identified in both the ingot and all the rod samples. Additionally, the $MnZn_{13}$ intermetallic phase was identified in the as-extruded and heat-treated rod samples. Figure 3b displays the weight fractions of each of the three intermetallic phases plotted as a function of heat treatment duration. The $MnZn_{13}$ phase is the most prevalent intermetallic prior to heat treatment but is substantially reduced after heat treatment. This phase decreases from 12.4 wt.% to 0.8 wt.% after 120 min. The content of the $ZrZn_{22}$ intermetallic phase decreases consistently throughout the different treatment durations until the 120-min heat treatment, at which point its concentration is nearly doubled. This indicates that the weight fraction of this phase begins to increase sometime after 60 min. The $Zn_{0.75}Ag_{0.15}Mn_{0.10}$ phase initially decreases but begins to increase after 40 min and its final concentration is just below its concentration prior to any heat treatment.

Mechanical Properties

The mechanical properties obtained from tensile and compression testing, including elongation to fracture (EL), ultimate tensile stress (UTS), tensile and compressive yield stress (YS), and elastic modulus (E), are summarized in Table 1, and the experimental curves are presented in Fig. 4. The results of the tensile testing demonstrate that the 390 °C heat treatment substantially increases the elongation to fracture of

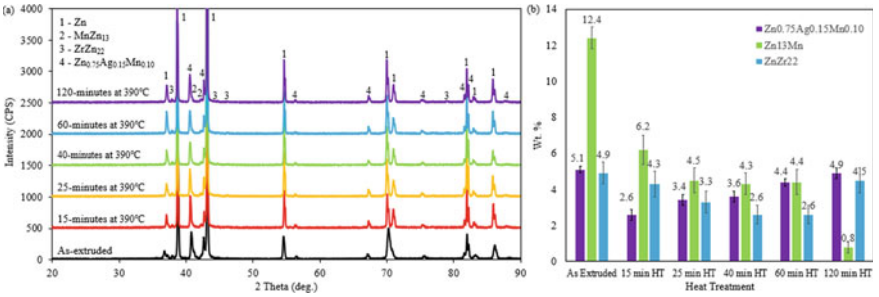

Fig. 3 **a** XRD spectra and **b** phase weight fraction data for rod in as-extruded and heat-treated conditions

the alloy at the cost of reduced strength. The alloy in the as-extruded state exhibits a UTS that meets the benchmark of 300 MPa that is required for materials in stent applications established by [8], but it does not meet the required 18–20% elongation to fracture. The three heat treatments do not display a significant difference in their mechanical properties, and while all their elongations at fracture meet the benchmark range, all UTS values fall short of the required value because of the increased grain size induced by the thermal treatment.

Similarly, the compression tests show a decrease in strength and increased ductility in all heat-treated conditions when compared with the as-extruded state. The results of mechanical testing suggest that the heat treatment temperature of 390 °C is too high for this series of zinc alloys. The decrease in strength is also correlated with decreased concentration of the $ZrZn_{22}$ and $MnZn_{13}$ phases, indicating the strengthening effects of these two intermetallics.

Table 1 Elongation to fracture (EL), ultimate tensile stress (UTS), and yield stress (YS) obtained from tensile testing, and YS and elastic modulus (E) with standard deviation obtained from compression testing

Sample condition	EL (%)	UTS (MPa)	Tensile YS (MPa)	Compressive YS (MPa)	E (MPa)
As-extruded	7.2	341	296	327 ± 1	6,200 ± 500
10 min, 390 °C	23.7	253	183	–	–
15 min, 390 °C	23.8	251	185	252 ± 2	5,960 ± 90
25 min, 390 °C	25.7	249	170	219 ± 4	6,000 ± 200
40 min, 390 °C	–	–	–	218 ± 3	6,000 ± 200
60 min, 390 °C	–	–	–	229	5,040
120 min, 390 °C	–	–	–	200	4,270

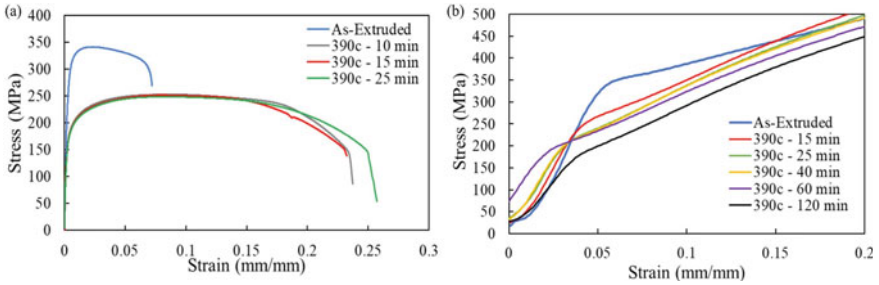

Fig. 4 Engineering stress versus strain **a** tensile and **b** compressive curves for as-extruded and heat-treated rod samples

Corrosion Properties

The corrosion resistance of the as-extruded and heat-treated alloy was evaluated with potentiodynamic corrosion measurements. A reduction in the corrosion rate of roughly 71% was observed from the as-extruded state (average corrosion rate with a standard deviation of 0.7 ± 0.1 mm/year) to the 15-min heat treatment (average corrosion rate with a standard deviation of 0.20 ± 0.02 mm/year).

The ideal corrosion rate of a degradable stent must be less than 0.02 mm/year in order to maintain mechanical integrity for the required 4–6 months of service [9, 14, 15]. The corrosion rates of the extruded rod both before and after heat treatment surpass this rate by an order of magnitude. The corrosion rate of this alloy appears to be substantially improved by thermal treatment, potentially related to the decreased content of the three intermetallic phases. The presence of intermetallics has been demonstrated to have a negative impact on the corrosion rates in magnesium alloys due to the enhancement of micro-galvanic corrosion [16]. Similar mechanisms may be responsible for the improved corrosion rate observed in this study, as the content of all intermetallics in the heat-treated specimen was lower when compared to the as-extruded.

Conclusions

In this study, the effectiveness of various heat treatment durations on a novel Zn-Ag-Mn-Cu-Zr-Ti alloy was investigated. This characterization included analysis of the microstructural evolution occurring from both hot extrusion and heat treatment, as well as an evaluation of mechanical and corrosive properties before and after heat treatment. Based on the results that were obtained, the following conclusions can be made:

- Hot extrusion results in significant refinement of microstructure. The average grain size of 70 ± 40 μm for the as-cast ingot was reduced by 87%.

- Increasing heat treatment duration at 390 °C beyond 10 min leads to a 10–20% increase in average grain sizes in the extruded rod.
- The alloy experiences ~50 MPa decrease in UTS as a result of thermal treatment at 390 °C but the ductility is improved from ~7 to 24–26%.
- Corrosion rate was found to be reduced from approximately 0.7 to 0.2 mm/year after 15-min heat treatment.
- The results of this study indicate that the temperature for heat treatment of the Zn-Ag-Mn-Cu-Zr-Ti alloy could be reduced below 390 °C. Further examination of the response to heat treatment at lower temperatures is required for the optimization of alloy processing for stent applications.

Acknowledgements U.S. National Institute of Health—National Heart, Lung, and Blood Institute grant 1R01HL144739-01A1 is acknowledged for funding this work.

References

1. Hanawa T (2009) Materials for metallic stents. J Artif Organs 12(2):73–79. https://doi.org/10.1007/s10047-008-0456-x
2. Heublein B (2003) Biocorrosion of magnesium alloys: a new principle in cardiovascular implant technology? Heart 89(6):651–656. https://doi.org/10.1136/heart.89.6.651
3. Grube E et al (2004) Six- and twelve-month results from first human experience using everolimus-eluting stents with bioabsorbable polymer. Circulation 109(18):2168–2171. https://doi.org/10.1161/01.CIR.0000128850.84227.FD
4. Bünger CM et al (2007) Sirolimus-eluting biodegradable poly-l-lactide stent for peripheral vascular application: a preliminary study in porcine carotid arteries. J Surg Res 139(1):77–82. https://doi.org/10.1016/j.jss.2006.07.035
5. Im SH, Jung Y, Kim SH (2017) Current status and future direction of biodegradable metallic and polymeric vascular scaffolds for next-generation stents. Acta Biomater 60:3–22. https://doi.org/10.1016/j.actbio.2017.07.019
6. Bünger CM et al (2007) A biodegradable stent based on poly(L-Lactide) and poly(4-hydroxybutyrate) for peripheral vascular application: preliminary experience in the pig. J Endovasc Ther 14(5):725–733. https://doi.org/10.1177/152660280701400518
7. Grabow N et al (2007) A biodegradable slotted tube stent based on poly(l-lactide) and poly(4-hydroxybutyrate) for rapid balloon-expansion. Ann Biomed Eng 35(12):2031–2038. https://doi.org/10.1007/s10439-007-9376-9
8. Bowen PK et al (2016) Biodegradable metals for cardiovascular stents: from clinical concerns to recent Zn-alloys. Adv Healthc Mater 5(10):1121–1140. https://doi.org/10.1002/adhm.201501019
9. Mostaed E, Sikora- M, Drelich JW, Vedani M (2018) Zinc-based alloys for degradable vascular stent applications. Acta Biomater 71:1–23. https://doi.org/10.1016/j.actbio.2018.03.005
10. Sun S, Ren Y, Wang L, Yang B, Li H, Qin G (2017) Abnormal effect of Mn addition on the mechanical properties of as-extruded Zn alloys. Mater Sci Eng A 701:129–133. https://doi.org/10.1016/j.msea.2017.06.037
11. ASTM (2004) Standard test methods for tension testing of metallic materials
12. ASTM (2019) Standard test methods of compression testing of metallic materials at room temperature
13. ASTM (2003) Standard test method for conducting potentiodynamic polarization resistance measurements

14. Mostaed E et al (2016) Novel Zn-based alloys for biodegradable stent applications: design, development and in vitro degradation. J Mech Behav Biomed Mater 60:581–602. https://doi.org/10.1016/j.jmbbm.2016.03.018
15. Bowen PK, Drelich J, Goldman J (2013) Zinc exhibits ideal physiological corrosion behavior for bioabsorbable stents. Adv Mater 25(18):2577–2582. https://doi.org/10.1002/adma.201300226
16. Zhang Y et al (2021) Influence of the amount of intermetallics on the degradation of Mg-Nd alloys under physiological conditions. Acta Biomater 121:695–712. https://doi.org/10.1016/j.actbio.2020.11.050